

RD50 Workshop, CERN,
14-16.11.2012

Electrical characterisation of heavily irradiated microstrip sensors

A.Chilingarov

Lancaster University, UK

On behalf of MCMD Collaboration

Layout

1. Introduction
2. CV and IV measurements
3. Strip capacitance
4. Interstrip resistance
5. Punch-through properties
6. Summary and conclusions

The talk is based on the Technical Note A.Chilingarov, “Post-irradiation Electrical Characterisation of the MCMD sensors”

https://ppes8.physics.gla.ac.uk/twiki/pub/DetDev/MCMD/protonIrrad_Char_postIrrad_AlexC_28June2012.pdf

1. Introduction

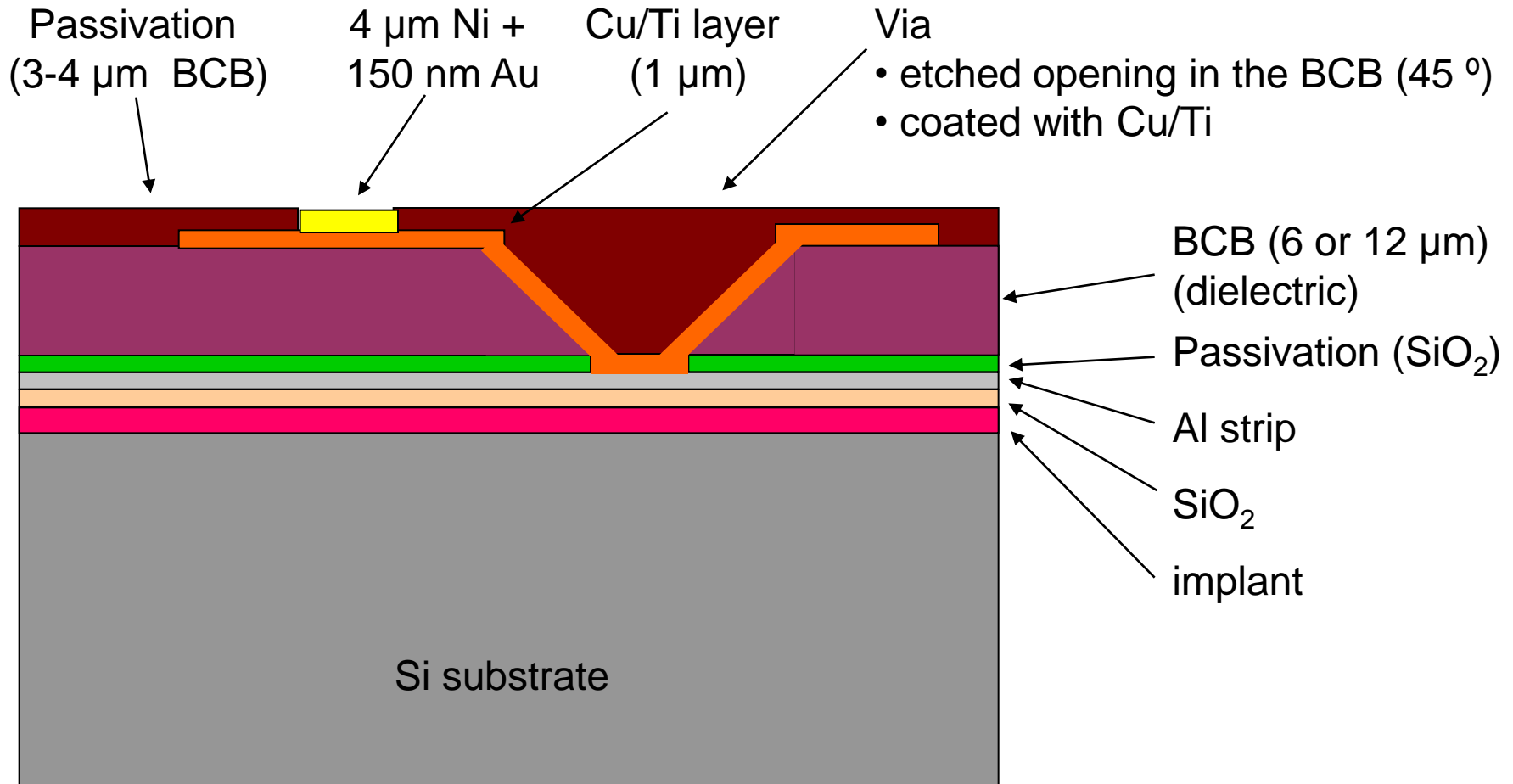
SCT sensors for ATLAS Upgrade will be built on *p*-type silicon. Radiation hardness of such sensors is much less known than that for traditional *n*-type material. Electrical characteristics of 4 microstrip *n-in-p* sensors irradiated by 1 MeV neutron equivalent fluences of 10^{13} , 10^{14} , 10^{15} and 10^{16} cm⁻² were measured.

The sensors also have a test structure in a form of a metal plane on 12 μm thick insulating layer covering the sensor. This technology (called MCMD) can allow building front-end hybrids directly on the sensors. Access to the sensor contacts is made through special Vias.

The sensors are 500 μm thick with 10x10 mm^2 sensitive area divided into 131 strips with 80 μm pitch and surrounded by a multi-guard-ring structure. Each strip has an AC coupled readout and is connected to the common bias rail via a polysilicon resistor of $\sim 2 \text{ M}\Omega$. The HV is applied to the sensor backside while the bias rail is grounded.

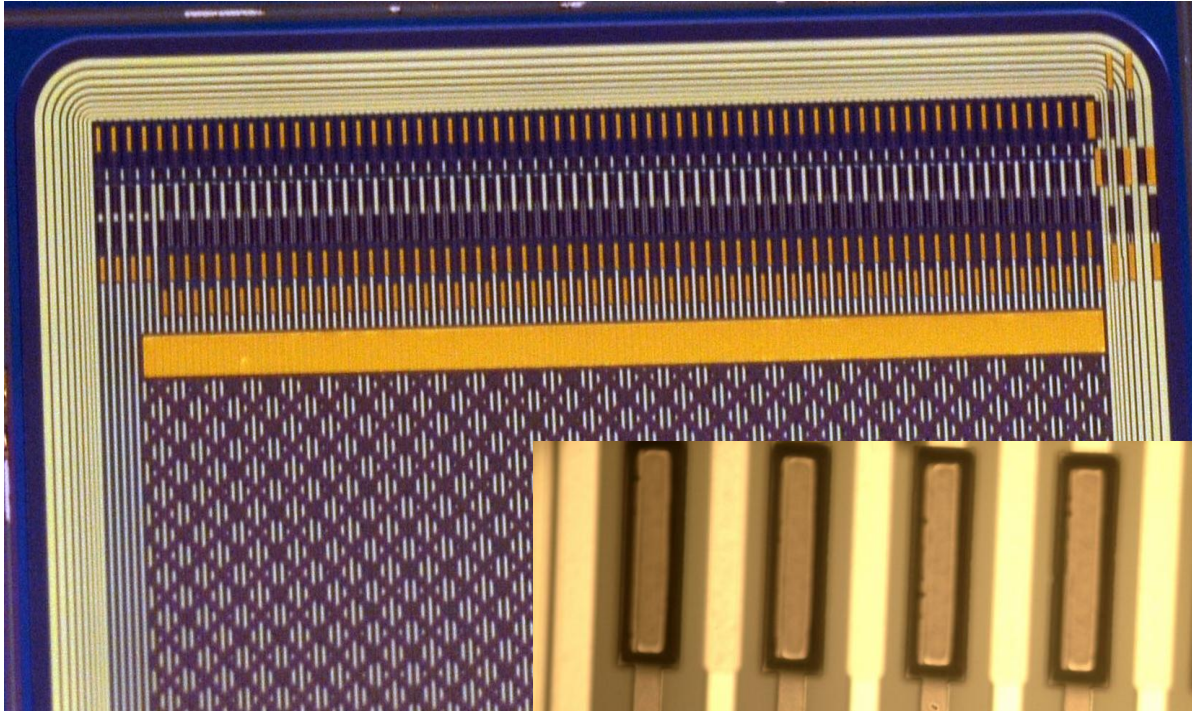
Metal plane above the sensor is a prototype of the ground plane (GNDP) of a future hybrid. It has a form of a mesh with 50% or 25% fill factor and line width of 30 μm or 80 μm . More information about MCMD detectors can be found at <https://ppes8.physics.gla.ac.uk/twiki/bin/view/DetDev/MCMD>

Cross-section of prototype run



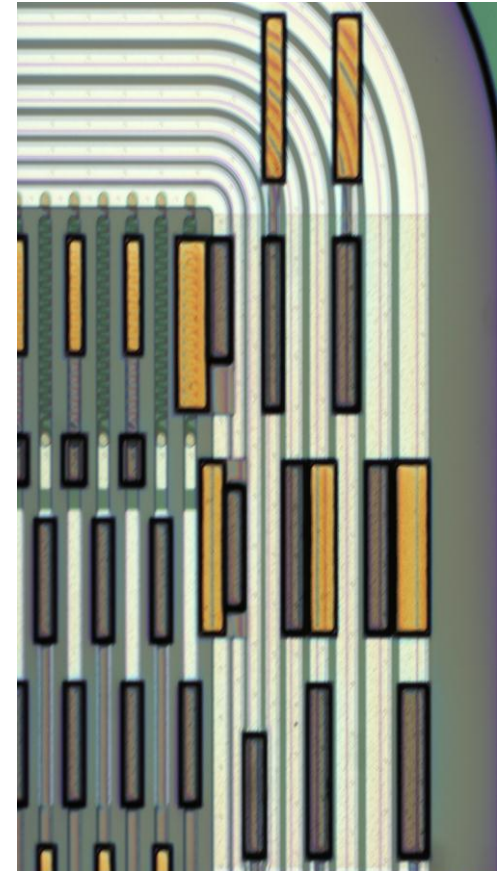
Implement the first layer of a fully functional hybrid: metal plane plus strip connections

Photos from prototype run



Sensor with meshed GND plane

Strip pad connections



Connections to bias and guard rings

Table 1. Sensors and their irradiation

Sensor #	Sensor name	Mesh type	1 MeV neq./cm ²	Dose, Mrad
1	x2y4	50% - 30μm	10 ¹³	1.4
2	x4y1	50% - 80μm	10 ¹⁴	14
3	x5y2	25% - 30μm	10 ¹⁵	140
4	x0y1	50% - 30μm	10 ¹⁶	1400

Sensors were produced by Micron Semiconductor. Interstrip isolation was achieved by a *p*-spray. Irradiation was made at Karlsruhe by 26 MeV protons. For calculation of the 1 MeV neutron equivalent fluence the hardness factor of 1.85 was applied.

Measurements were made with sensors mounted in the test frames and placed inside the cool box with controlled temperature and humidity.

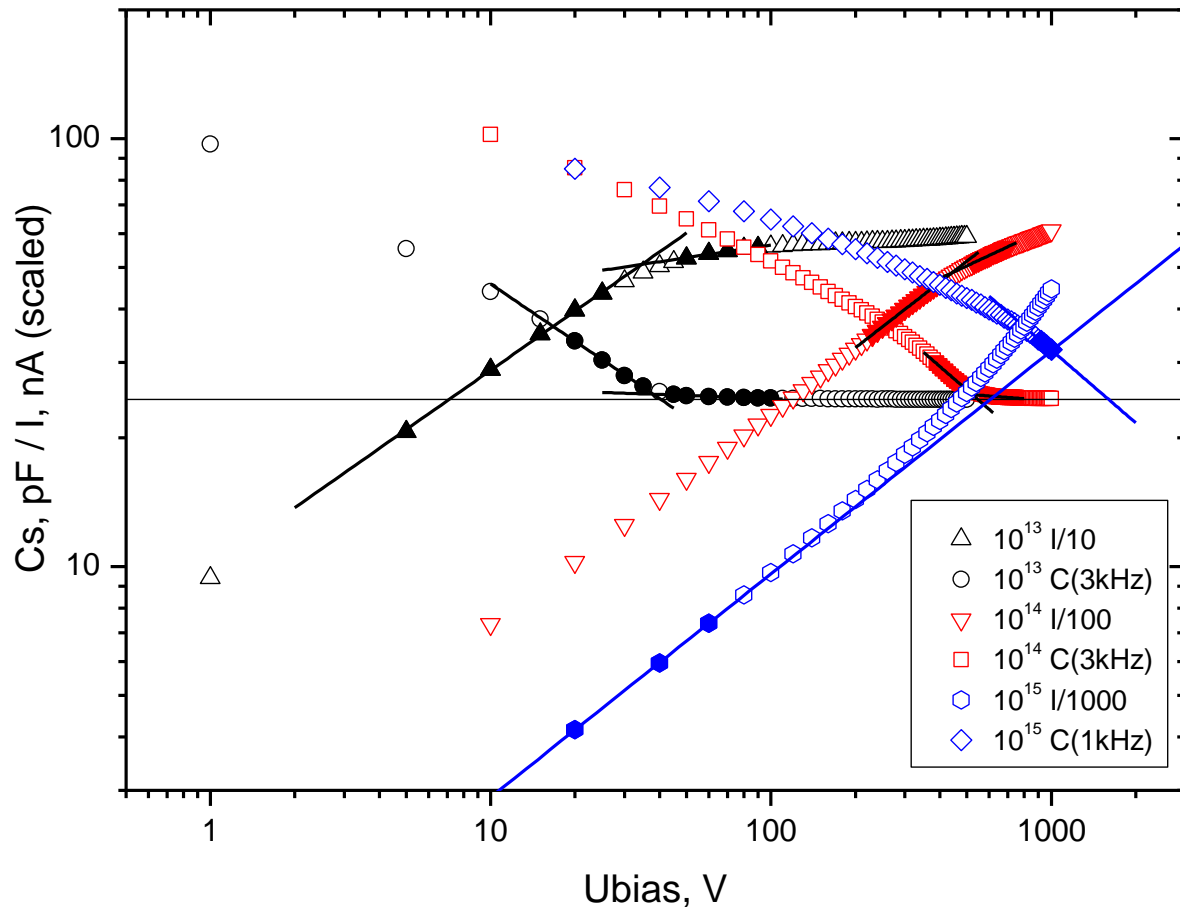
2. CV and IV measurements

Both CV and IV characteristics were measured in the same bias ramp.

Measurements were made with the innermost guard ring grounded. The total current, I_t , and that through the sensor centre, I_c , were measured.

The capacitance was measured between the bias rail and the backside in C_s - R_s mode at the frequency of 1 or 3 kHz.

Measurement temperature was either -20°C or -32°C .



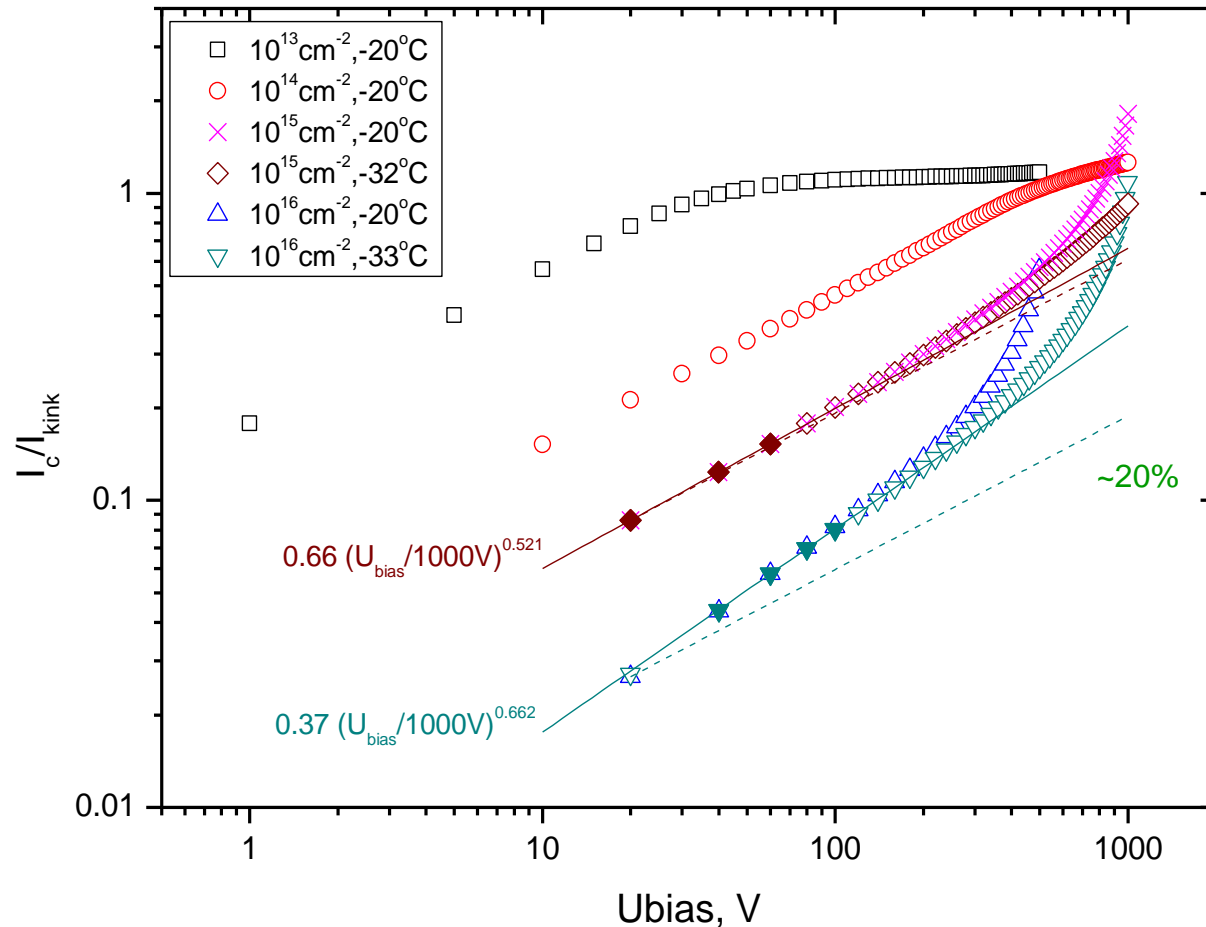
The depletion voltage, V_d , was found to be $\sim 35\text{V}$ and $\sim 500\text{V}$ for the sensors irradiated by 10^{13} and 10^{14} n/cm^2 respectively. Thus for the 10^{15} and 10^{16} irradiations one can expect V_d of ~ 5 and 50kV .

For the sensor irradiated by 10^{15} n/cm^2 the V_d was estimated as ~ 1.6 kV from the CV curve extrapolation to the C value found for the other two sensors

C-V and I_c -V curves for detectors irradiated by 10^{13} , 10^{14} (at -20°C) and 10^{15} n/cm^2 (at -32°C). The currents are corrected to -20°C and divided by factors 10, 100 and 1000 to simplify the comparison. The -20°C current at the kink position vs. fluence can be parameterised as $4825 \text{ nA} \cdot (F/10^{14} \text{ n/cm}^2) + 29 \text{ nA}$.

For the sensors #1 and #2 the current below the kink grows as $U^{1/2}$.

At low volts (filled points) where sensor self-heating can be neglected the currents for sensors #3 and #4 grow as $U^{0.52}$ and $U^{0.66}$ respectively. Then I_c/I_{kink} extrapolation to unity gives V_d of 2.2kV and 4.5kV. Scaling of the first points by the $U^{1/2}$ gives 2.7kV and 28kV. All values are lower than a naïve scaling from the sensor #2: 5 and 50kV.



All currents are corrected to -20°C and normalised by their measured or calculated values at the kink position. For the sensors #3 and #4 the scaling from -32°C to -20°C was made using low bias points measured for the same sensors at -20°C .



3. Strip capacitance

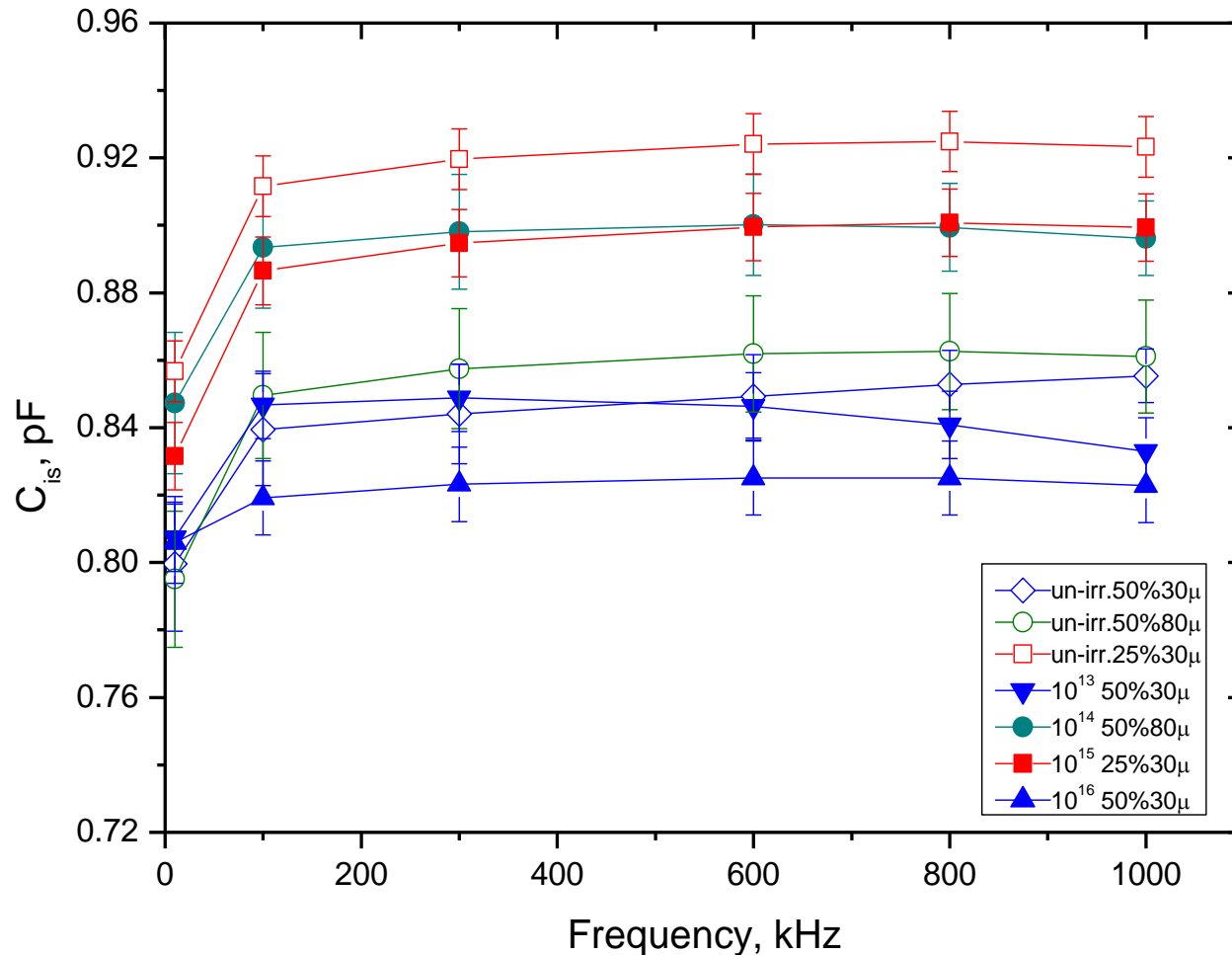
3.1 Capacitance to the neighbouring strips, C_{is}

Interstrip capacitance gives a main contribution to the capacitive load of the front-end electronics and thus is a major source of noise. It was measured as a capacitance, C_{is} , between a strip and its two nearest neighbour strips connected together.

The presence of GNDP connected to the ground affects the C_{is} value. Therefore the irradiated sensors were compared with non-irradiated ones having the same type of mesh.

For 1 cm long strip the C_{is} is ~ 0.8 pF. Stray capacitances are of the same order and were measured for each test frame individually at every used temperature. Their variation ~ 0.02 pF due to reconnections of external cables was a major source of uncertainty for C_{is} .

The C_{is} was first measured as a function of bias (usually quite weak) and then allowed to stabilise at the maximum U_{bias} before its final value was taken.



The C_{is} is practically independent of frequency between 200 and 1000 kHz.

Within uncertainties there is no increase of C_{is} with irradiation up to the highest fluence of 10^{16} n/cm 2 .

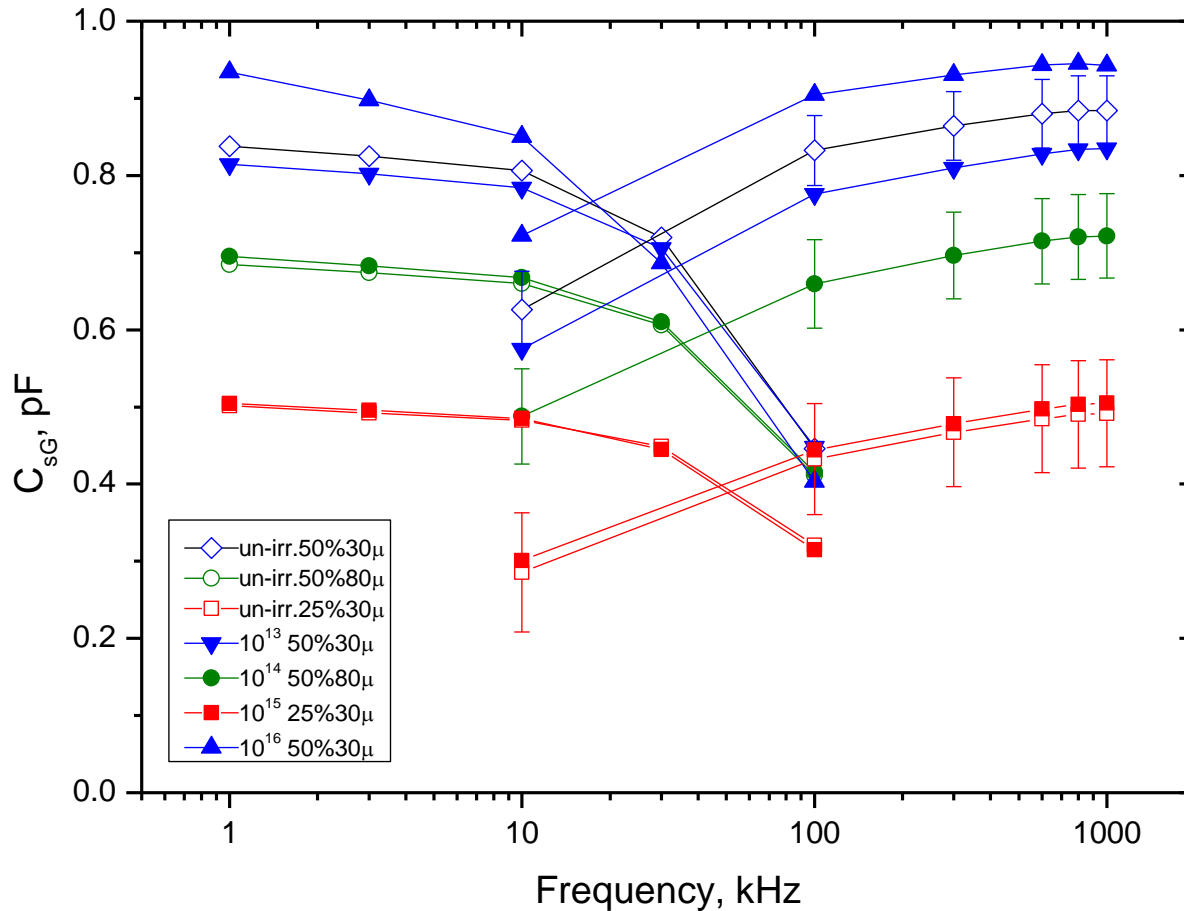
C_{is} vs. measurement frequency for un-irradiated (open symbols) and irradiated (filled symbols) sensors. U_{bias} = 500V for non-irradiated sensors and 10^{13} n/cm 2 fluence, 1000V for 10^{14} , 800V for 10^{15} and 10^{16} n/cm 2 fluences.

3.2 Capacitance to the GNDP, C_{sG}

The capacitance between a strip and GNDP, C_{sG} , adds up to the capacitive load. For the investigated sensors with 12 μm BCB thickness it is of the same order as C_{is} and increases with the mesh density.

One way to find C_{sG} is to measure the capacitance from the bias rail (BR) to GNDP and divide it by the number of strips. This method gives very accurate C_{sG} value but can work well only for low measurement frequencies because of the presence of bias resistor of $\sim 2\text{M}\Omega$ between a strip and BR.

Another method is to measure capacitance between n adjacent strips connected together and GNDP. It works well for high frequencies (more relevant for fast electronics) but has a significant systematic uncertainty. Since for practical reasons the number of tested strips, n , can't be large the proper subtraction of the C_{is} contribution is difficult. The ways to solve this problem are described in the Technical Note quoted at slide 2.



For the sensor irradiated by 10^{16} n/cm² the C_{sG} is by $\sim 10\%$ higher than before irradiation. For 3 other fluences no effect of irradiation is visible.

Within systematic uncertainties the high frequency values agree well with more precise low frequency data.

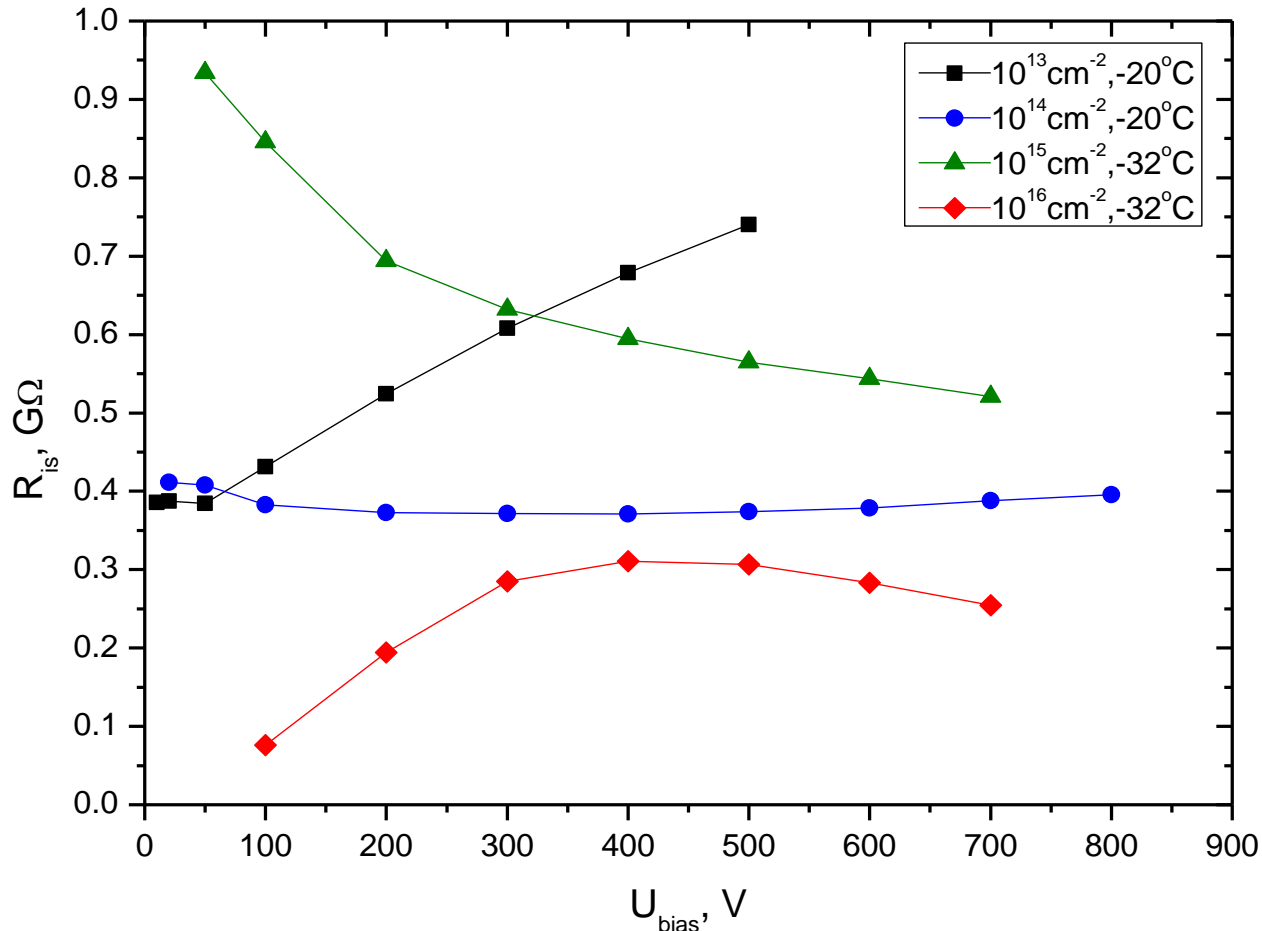
C_{sG} vs. measurement frequency. Low frequency data are more precise while high frequency are more relevant but with a significant systematic uncertainty shown for several sensors by the error bars. U_{bias} is the same as in C_{is} measurements.

4. Interstrip resistance, R_{is}

Interstrip resistance was measured by applying test DC potential to a strip implant and measuring the voltage induced by it at an adjacent strip. The method is described in detail in the Note **RD50-2009-01** A.Chilingarov, “Interstrip resistance measurement”.

Due to layout constraint only every second implant strip was accessible. As explained in the above Note the maximum measurable R_{is} in this case is $\sim 1\text{G}\Omega$ and limited by non-zero resistance of the sensor bias rail.

Measurement temperature was -20°C for the sensors irradiated by 10^{13} and 10^{14} n/cm² and -32°C for more heavily irradiated sensors.



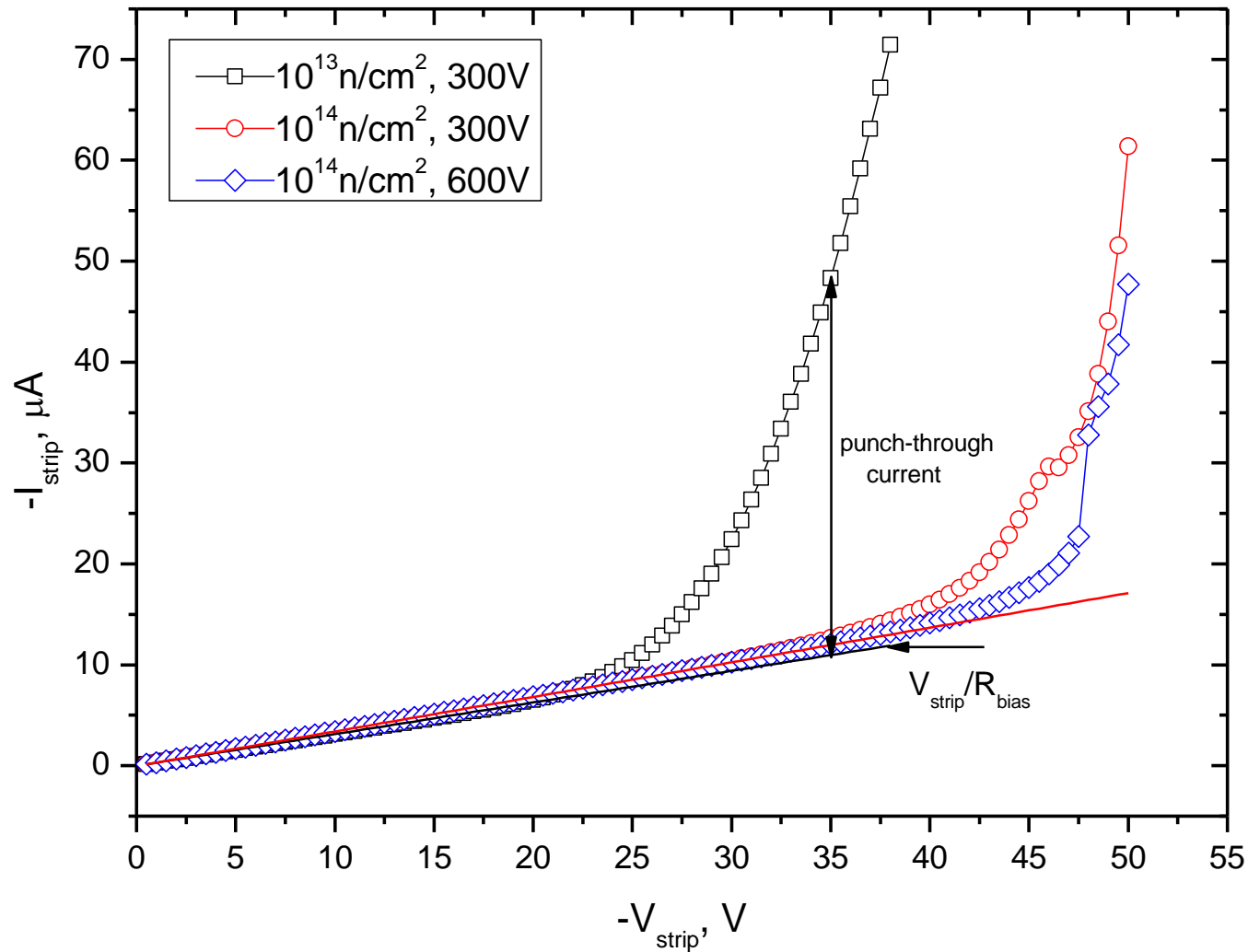
Interstrip resistance, R_{is} , as a function of bias. For $U > 100 \text{ V}$ the $R_{is} > 100 \text{ M}\Omega$, i.e. well above $R_{bias} \sim 1 \text{ M}\Omega$ and therefore harmless.

5. Punch-through properties

The sensors have no special structures for punch-through protection. The punch-through (PT) develops simply via 19 μm gap between the strip implant edge and the bias rail (BR) at both strip ends.

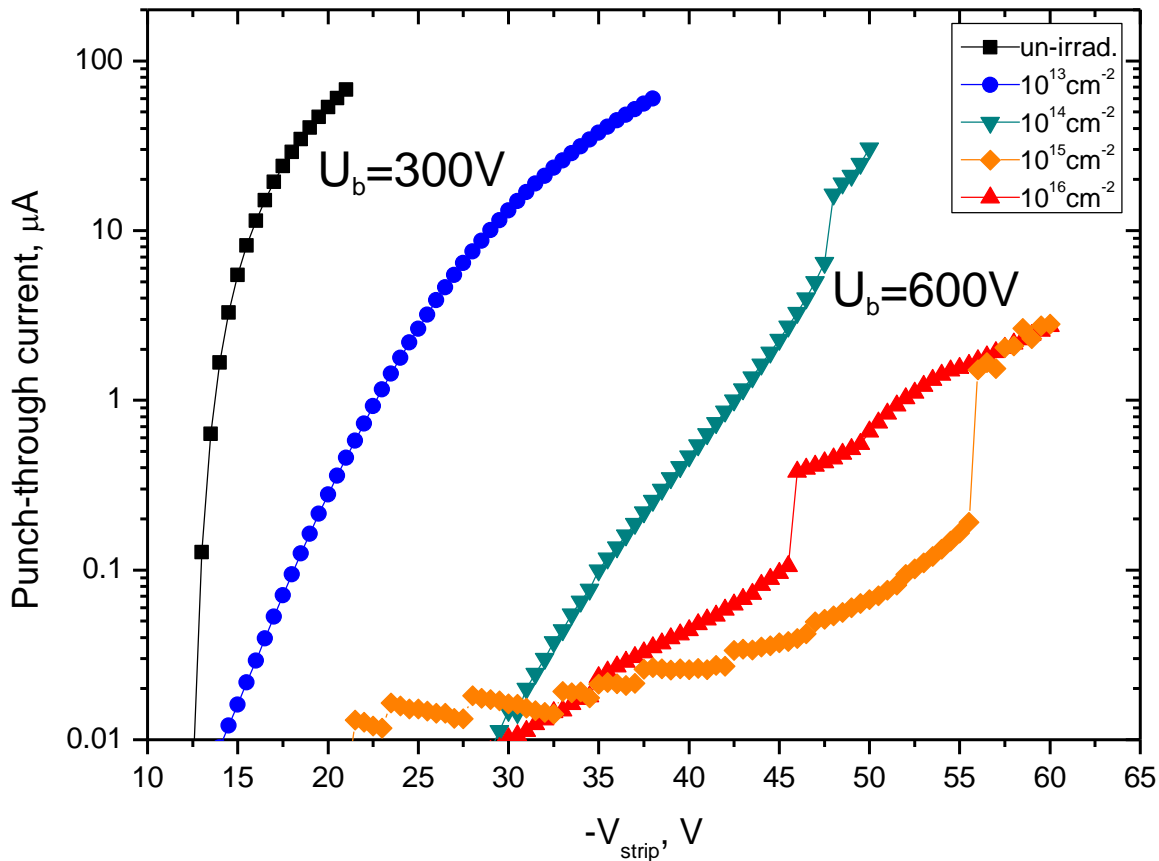
PT was studied by applying negative DC potential to a strip implant and measuring the resulting current. At low volts the current flows to BR only through the bias resistor and grows linearly with voltage. At higher volts the PT current appears as a component additional to the linear rise.

Typically the PT current grows very steeply with voltage above the onset value thus preventing a building up of high potential at the strip implant by an accidental high current through the sensor e.g. because of the beam loss.



Punch-through current measurements for the sensors irradiated by 10^{13} and 10^{14} n/cm^2 at bias of 300V and 600V .





Irradiation increases the PT onset voltage and decreases the IV steepness above the onset.

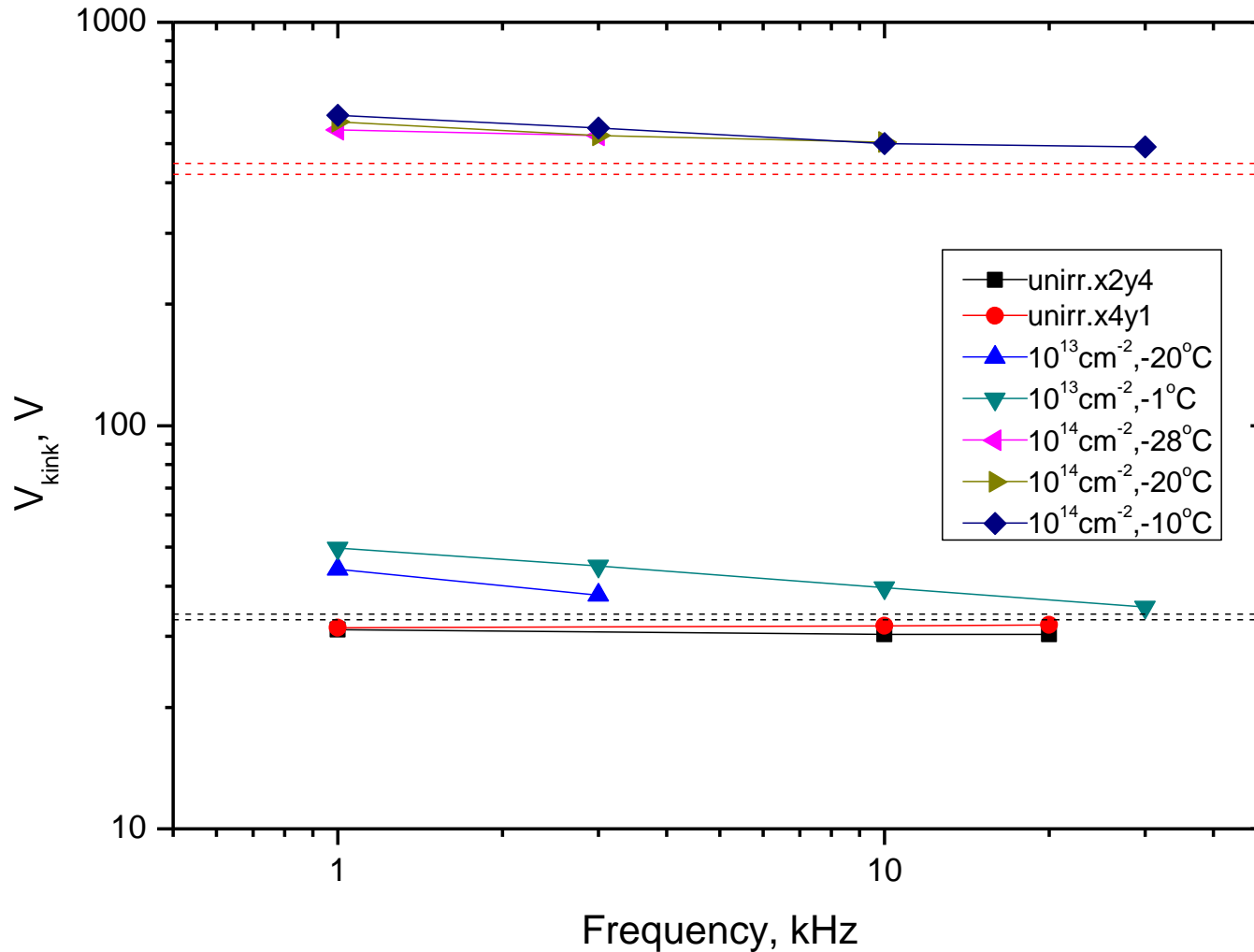
For an assumed safe potential of 50V the PT can drain from the strip >100µA for the fluence below 10¹⁴ n/cm² but <1µA for the fluence ≥ 10¹⁵ n/cm². Dedicated PT structures are needed to provide PT protection after high fluence.

The PT current vs. test potential for un-irradiated and 4 irradiated sensors. The current is expected first to grow exponentially and then start saturating.

6. Summary and conclusions

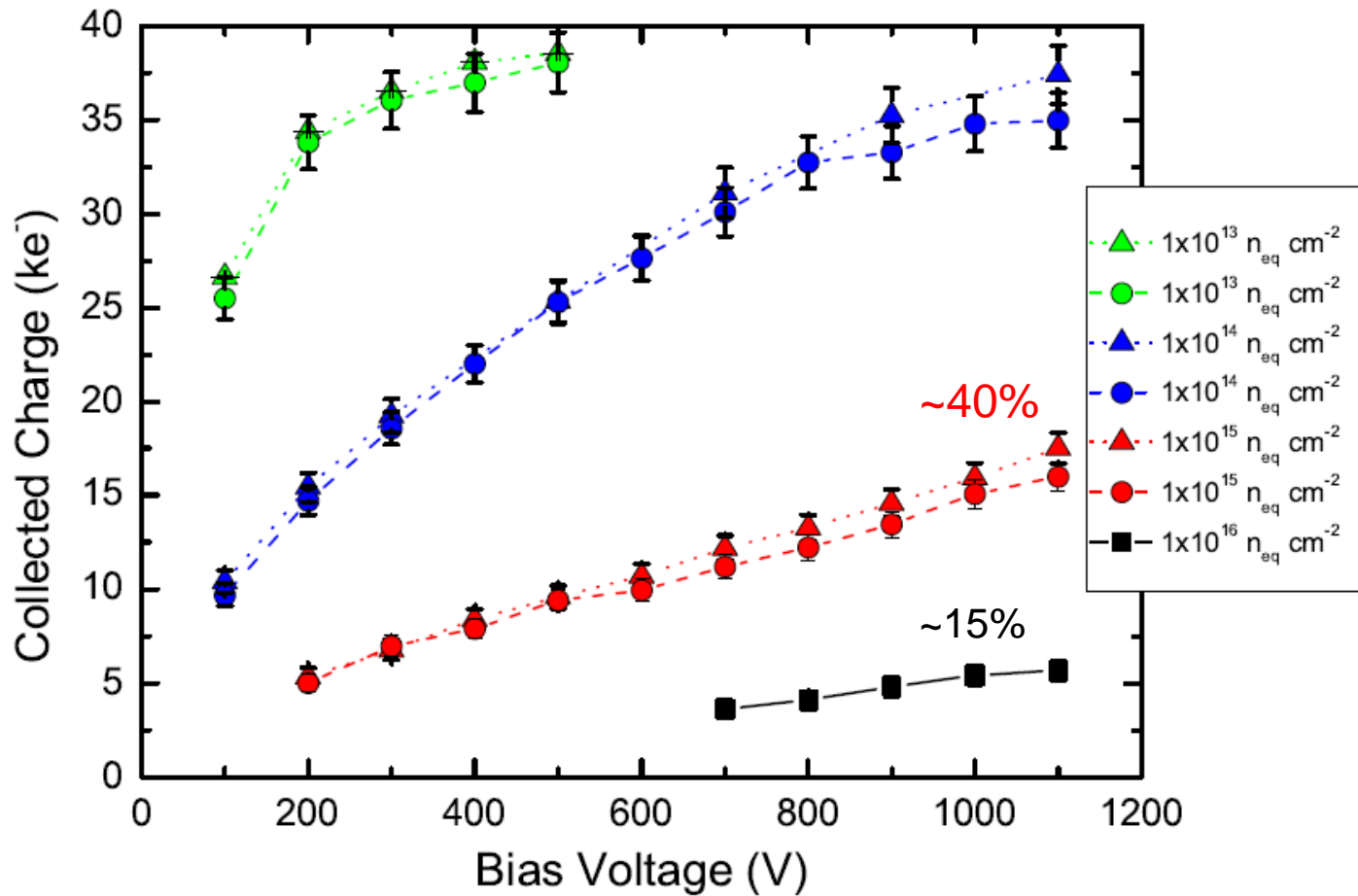
1. The current and depletion voltage increase with fluence as expected up to 10^{14} n/cm². Beyond this the current growth with bias becomes faster indicating the carrier extraction from the neutral bulk.
2. The interstrip capacitance and that from a strip to GNDP do not change with irradiation.
3. Interstrip resistance remains very high up to 10^{16} n/cm² fluence.
4. The sensors have no special PT structures but a simple gap of 19 μ m works well up to the fluence between 10^{13} and 10^{14} cm⁻². Special PT structures have to be implemented for similar ability at higher fluences.

Backup slides

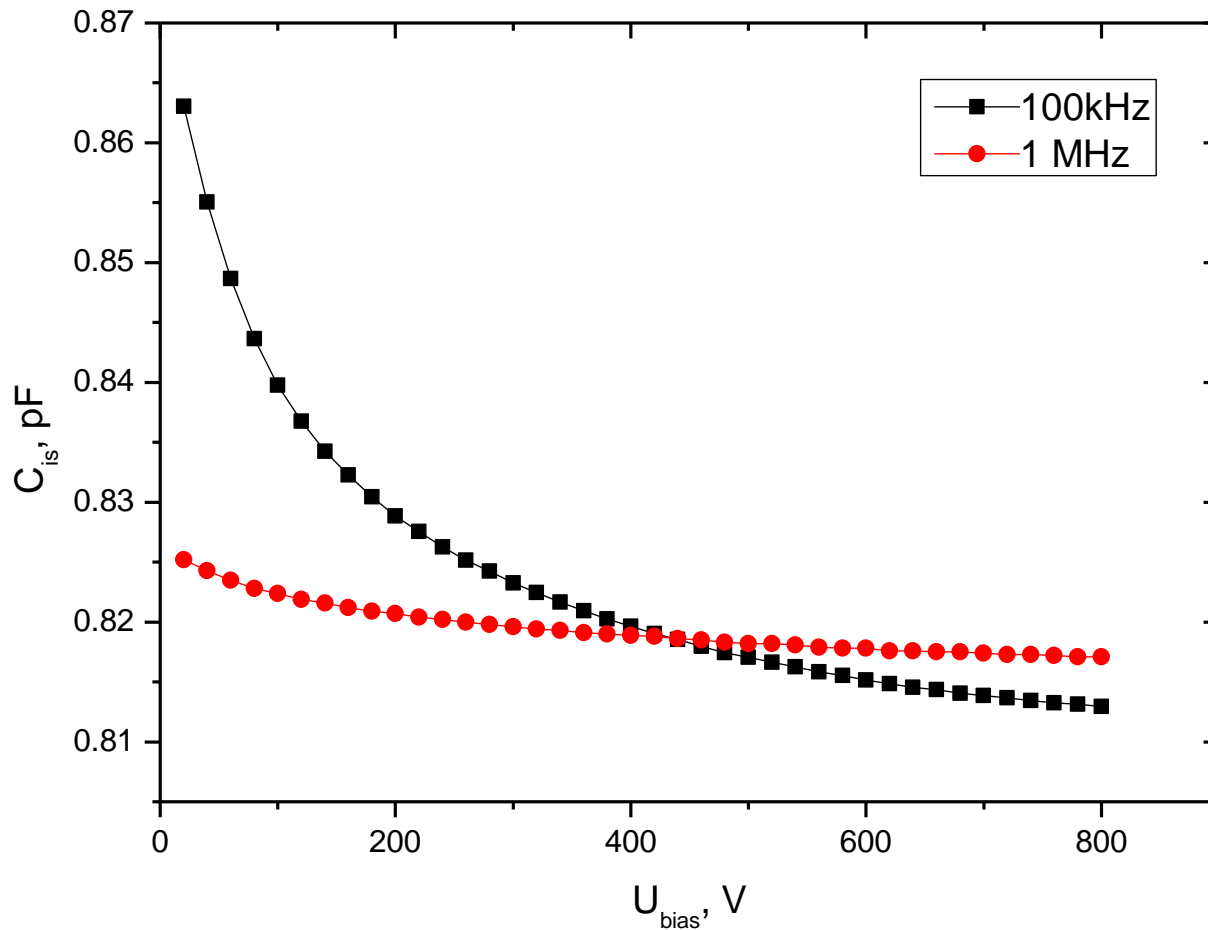


Full depletion voltage estimated as “kink” position in C-V plots vs. measurement frequency (points) and I_c -V plots (dotted lines showing lower and upper limits).

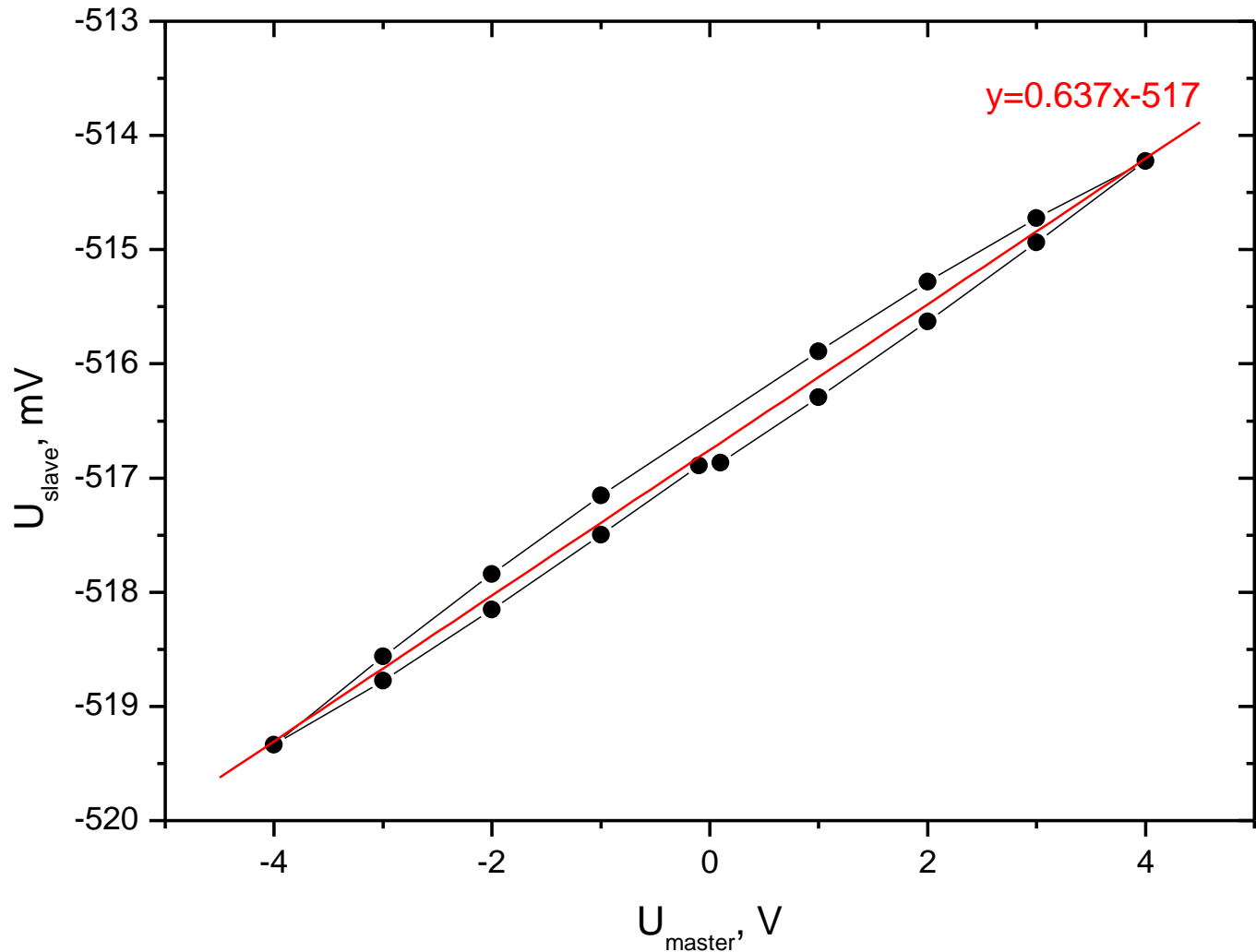




CCE measurements made at Liverpool University using Sr⁹⁰ beta source.



C_{is} - V at frequencies of 100kHz and 1 MHz for the sensor irradiated by 10^{16} n/cm².



$$R_{is} = R_{bias} / S^{1/2};$$

$$S = dU_{slave} / dU_{master} = 6.4 \cdot 10^{-4};$$

$$R_{bias} = 4.8 \text{ M}\Omega \rightarrow$$

$$R_{is} = 190 \text{ M}\Omega.$$

R_{is} measurement at $U_{bias} = 200\text{V}$ in the sensor irradiated by 10^{16} n/cm^2 : potential U_{slave} induced at the next neighbour strip by the test potential U_{master}

